Energy & Environmental Science

Cite this: *Energy Environ. Sci.*, 2012, **5**, 6136

www.rsc.org/ees

PAPER

Hydrogen evolution catalyzed by MoS_3 and MoS_2 particles†

Heron Vrubel, Daniel Merki and Xile Hu*

Received 5th October 2011, Accepted 12th December 2011
DOI: 10.1039/c2ee02835b

Amorphous MoS_3 particles are prepared using a simple chemical method. Several deposition techniques are developed to fabricate electrodes loaded with MoS_3 particles. These electrodes are highly active for hydrogen evolution. The catalytically active species appear to be reduced molybdenum sulfide that contains disulfide ligands. The MoS_3 particles are annealed to form polycrystalline and single crystalline MoS_3 and MoS_2 particles. These particles, as well as commercial MoS_2 micro-crystals, show inferior catalytic activity compared to the amorphous MoS_3 particles.

1. Introduction

An attractive method to store solar energy is to split water using sunlight, producing hydrogen and oxygen fuels. Hydrogen evolution, or the reduction of protons to form hydrogen, is the reductive half reaction of water splitting. This reaction requires catalysts. There is now renewed interest in the development of efficient and non-precious hydrogen evolution catalysts.[1–3] Despite intense research, few synthetic catalysts are known to operate in water, give a high current density at a low overpotential (η), and have a quantitative current efficiency.[2,3] MoS_2 single crystals and nanoparticles, and related metal sulfide nanoparticles, have been shown as promising hydrogen evolution catalysts.[3–6] These catalysts are normally prepared at a high temperature, high vacuum, and with special instrumentation. The process can be costly and energy intensive. We recently discovered that amorphous MoS_x ($x = 2$, 3) films were excellent hydrogen evolution catalysts.[6,7] The films were made by electropolymerization of $[MoS_4]^{2-}$ at room temperature and ambient pressure. Compared to MoS_2 nanoparticles, the MoS_x films have a more favorable activity/cost trade-off.[6] Shortly after, a solution method to deposit amorphous MoS_3 catalysts on CdSe-seeded CdS nanorods under mild conditions (90 °C) was also reported.[8]

With respect to the MoS_x films developed by us, the fabrication method poses a constraint in the practical implementation of these catalysts: the films have to be made by electrodeposition at 0.3 to −0.8 V *vs.* SHE.[7] Electrodes that are not stable in such an electrochemical window are thus not suitable substrates. Many semiconducting and non-conducting substrates cannot be used neither.

The shortcomings of the MoS_x films can be overcome if the amorphous MoS_x catalysts can be produced chemically and in a large quantity. Various deposition methods can then be applied to assemble the catalysts onto a wide range of substrates. Herein, we describe the chemical preparation of amorphous MoS_3 particles and their catalytic activity for HER. The amorphous MoS_3 particles are annealed to form crystalline forms of MoS_3 and MoS_2 particles. The catalytic property of the latter particles and of commercial MoS_2 micro-crystals is measured and compared to that of amorphous MoS_3 particles.

Laboratory of Inorganic Synthesis and Catalysis, Institute of Chemical Sciences and Engineering, Ecole Polytechnique Fédérale de Lausanne (EPFL), ISIC-LSCI, BCH 3305, Lausanne, CH 1015, Switzerland. E-mail: xile.hu@epfl.ch; Fax: +41 216939305; Tel: +41 216939781

† Electronic supplementary information (ESI) available: figures and tables. See DOI: 10.1039/c2ee02835b

Broader context

Hydrogen evolution catalysts are important components of photoelectrochemical water splitting devices. The scale of the world's demand for energy calls for non-precious HER catalysts. Molybdenum sulfide catalysts are promising candidates in this regard, because they are made of relatively abundant and inexpensive elements. In this paper, we describe a simple solution-based method to prepare amorphous MoS_3 particles under mild conditions. We develop several techniques to fabricate MoS_3-modified electrodes which exhibit high HER activity. We carry out a structure activity study to show that among various molybdenum sulfide species, amorphous MoS_3 particles have the highest catalytic activity. The work advances the development of molybdenum sulfide-based HER catalysts.

2. Results and discussion

2.1 Synthesis and characterization of amorphous MoS_3 particles

Amorphous MoS_3 particles are normally prepared by acidification of tetrathiomolybdate solutions.[9] We found that MoS_3 could be obtained upon acidification of a solution of MoO_3 and Na_2S, making the synthesis more economical. In a typical procedure, molybdenum trioxide was added to an aqueous solution containing 5 equiv. of sodium sulfide to form a bright yellow solution. The solution was acidified with a 6.0 M aqueous HCl solution to pH = 4. The solution was then boiled for 30 minutes and cooled to room temperature to give a dark paste. The paste was oven dried for 12 h at 80 °C to give a black vitreous solid that was ground into MoS_3 powder with a mortar. The dark paste was also converted into a MoS_3 sol by suspending and sonicating in acetone for several minutes.

The XPS spectra of MoS_3 (Fig. 1 and S1, ESI†) are similar to those of known MoS_3 samples.[10,11] The survey spectrum (Fig. S1, ESI†) shows predominantly peaks from Mo and S, although some peaks of C and O from adventitious impurities are also visible. The Mo 3d spectrum indicates that the Mo ion is in the 4+ oxidation state, with a Mo $3d_{5/2}$ binding energy of 228.6 eV. The S 2p spectrum consists of two doublets with S $2p_{2/3}$ energies of 162.0 and 163.3 eV. The relative intensity of the doublets is 5 : 4, favoring the doublet with a higher binding energy. The spectrum suggests the existence of both S^{2-} and S_2^{2-} ligands. The same spectrum was observed previously on amorphous MoS_3.[10] It was suggested that the doublet with the higher binding energy might be attributed to bridging S_2^{2-} and/or apical S^{2-} ligands. The doublets with the lower energy might be attributed to terminal S_2^{2-} and/or S^{2-}. Because different kinds of sulfur ligands have similar binding energies in XPS, it is not possible to quantify the ratio of these sulfur ligands.[10] However, the spectrum of MoS_3 is significantly different from those of MoS_2 and other molybdenum sulfide species.[10] Thus, based on the similarity in the XPS spectra of the molybdenum sulfide samples prepared here and known MoS_3 materials, these samples are assigned as MoS_3. This is confirmed by the Mo to S ratio of 1 to 3 determined by XPS quantification. Fig. 2 shows the TEM images of the particles. According to electron diffraction study, the particles are amorphous and non-crystalline (no diffraction pattern observed).

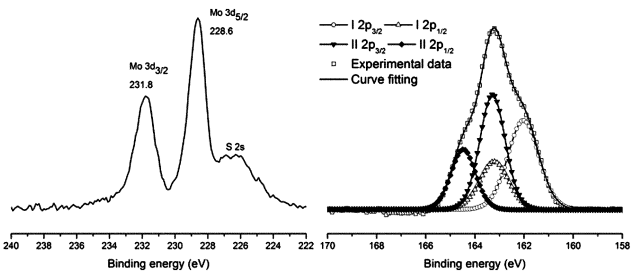

Fig. 1 XPS spectra of the MoS_3 particles. (Left) Mo 3d and S 2s region. (Right) S 2p region; binding energies (eV): doublet I $2p_{3/2}$, 162.0; $2p_{1/2}$, 163.2; doublet II $2p_{3/2}$, 163.3; $2p_{1/2}$, 164.5.

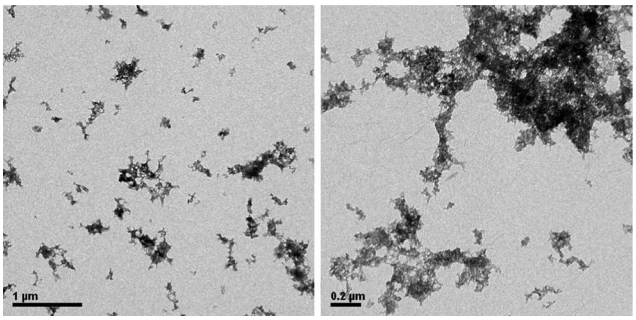

Fig. 2 TEM images of the MoS_3 particles.

2.2 Fabrication and catalytic property of MoS_3-modified electrodes

2.2.1 Electrodes made by drop-casting. To test the catalytic activity for hydrogen evolution, the MoS_3 particles need to be incorporated into an electrode. We first applied the method of drop-casting. The MoS_3 sol was used as the source of MoS_3. A modified electrode could be prepared by first drop deposition of the MoS_3 sol on the electrode surface and subsequent evaporation of the solvent. The amount of MoS_3 was estimated according to the concentration of the sol. Both FTO and glassy carbon were used as the substrates.

Fig. 3 shows the SEM images of a MoS_3-modified FTO electrode assembled by drop-casting. The MoS_3 particles cluster together into aggregated wires. The surface appears rough. The catalytic property of the electrode toward HER was studied by polarization measurements. The activity of a freshly prepared electrode increases during the first several polarization scans, until a stable current is observed (normally after six scans; Fig. S2, ESI† and *vide infra*). Presumably a reorganization and/or activation process occurs during these scans to reach the maximum activity (see Section 2.3 for discussion). Fig. 4 shows the (stable) polarization curves of the modified electrodes at pH = 0.

The modified FTO electrodes show high activity for hydrogen evolution. Non-baseline currents were already observed at η = 100 mV. Up to a loading of 53 μg cm^{-2} MoS_3, a higher loading results in a higher current at the same potentials. For an electrode with a loading of 53 μg cm^{-2} MoS_3, the current densities are 0.18 and 1.1 mA cm^{-2} at η = 150 and 200 mV, respectively. When the loading is higher than 53 μg cm^{-2} MoS_3, the current densities are lower. The Tafel slopes are in the range of 52 to 61 mV per decade (Table S1, ESI†).

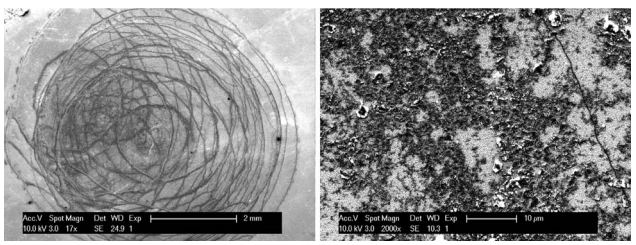

Fig. 3 SEM images of a MoS_3-modified FTO electrode prepared by drop-casting. Overview of the modified area (left) and deposited MoS_3 at a higher magnification (right).

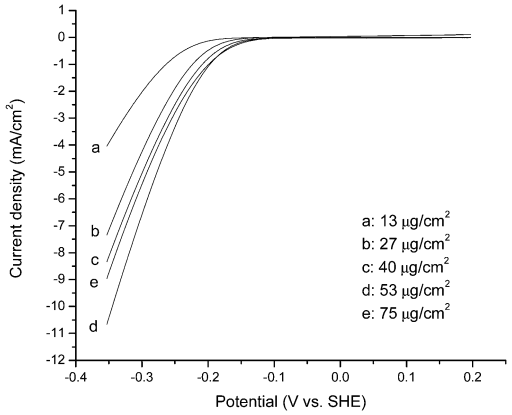

Fig. 4 Polarization curves of drop-cast MoS_3-modified FTO electrodes recorded at pH = 0 (1.0 M H_2SO_4); scan rate: 5 mV s^{-1}.

The MoS_3 particles were then deposited on a glassy carbon electrode using the same drop-casting method. Fig. 5 (top) shows the (stable) polarization curves of the modified electrodes at pH = 0. The dependence of HER rate on the loading of MoS_3 can be observed. The optimal loading is 32 μg cm^{-2}. If the loading is higher, a lower catalytic activity is observed. This is better illustrated in Fig. 5 (bottom), which plots the loading-dependent current densities at $\eta = 150$ and 200 mV. The current densities at the optimal loading are 0.35 and 2.3 mA cm^{-2} at $\eta = 150$ and 200 mV, respectively.

Tafel slopes of 41–63 mV per decade are found for these MoS_3/glassy carbon electrodes (Table 1). At a low loading, the Tafel slope is close to 40 mV per decade, the same as the value obtained on MoS_x films.[7] A Tafel slope of 50 to 60 mV per decade is found for electrodes with higher loading of MoS_3. The increased Tafel slope is probably due to decreased efficiency in electron and proton transfer when the loading of catalyst is higher. Thus, the higher catalytic activity associated with a higher catalyst loading is counter-played. An optimal loading ensues.

To improve the electron transfer to catalyst, multiwalled carbon nanotubes (MWCNTs) were added to the MoS_3 sol as a conducting additive. Fig. 6 shows the dependence of HER activity on the loading of MWCNT. In general, a higher loading of MWCNT leads to a higher current density. Tafel analysis shows that the Tafel slope decreases from about 50 mV per decade to 40 mV per decade when MWCNT is added to the MoS_3 sol (Table 2). Under these conditions, the current densities are 0.50 and 4.8 mA cm^{-2} at $\eta = 150$ and 200 mV, respectively (21 μg cm^{-2} of MoS_3).

2.2.2 Electrodes made by spray-casting. As drop-casting produces a MoS_3 film that is rough and aggregated (Fig. 3), we sought to produce films with better morphology using spray-casting. Fig. 7 shows the SEM images of a MoS_3-modified FTO

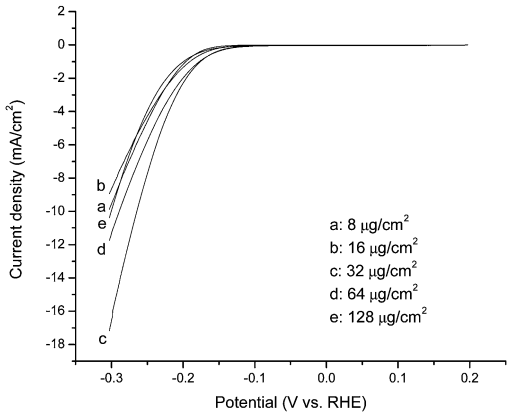

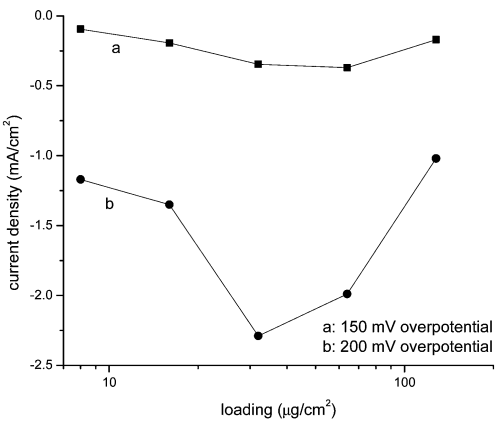

Fig. 5 (Top) Polarization curves of drop-cast MoS_3-modified glassy carbon electrodes recorded at pH = 0 (1.0 M H_2SO_4); scan rate: 5 mV s^{-1}. (Bottom) Loading-dependence of current densities.

Table 1 HER activity of drop-cast MoS_3-modified glassy carbon electrodes according to polarization measurements

Loading/ μg cm^{-2}	log j_0 (log [mA cm^{-2}])	Tafel slope/ mV per decade	$j_{\eta=150}$/ mA cm^{-2}	$j_{\eta=200}$/ mA cm^{-2}
8	−4.7	41[a]	0.094	1.2
16	−3.6	51[b]	0.19	1.4
32	−3.2	54[c]	0.35	2.3
64	−3.0	60[d]	0.37	2.0
128	−3.2	63[e]	0.17	1.0

[a] Determined at η = 135–175 mV. [b] Determined at η = 125–168 mV. [c] Determined at η = 120–175 mV. [d] Determined at η = 120–170 mV. [e] Determined at η = 133–185 mV.

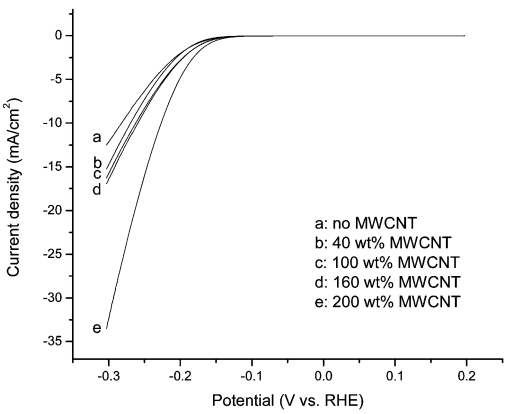

Fig. 6 Polarization curves of drop-cast MoS_3-modified glassy carbon electrodes blended with MWCNTs. The measurements were conducted at pH = 0 (1.0 M H_2SO_4); MoS_3 loading: 21 μg cm^{-2}; scan rate: 5 mV s^{-1}.

Table 2 Influence of MWCNT on the HER activity of drop-cast MoS_3-modified glassy carbon electrodes, according to data in Fig. 6

MoS_3/MWCNT (weight ratio)	log j_0 (log [mA cm^{-2}])	Tafel slope/ mV per decade	$j_{\eta=150}$/ mA cm^{-2}	$j_{\eta=200}$/ mA cm^{-2}
No MWCNT	−3.6	49[a]	0.28	2.0
1 : 0.4	−4.2	43[b]	0.22	2.1
1 : 1	−4.0	43[c]	0.37	2.8
1 : 1.6	−4.1	41[d]	0.35	2.9
1 : 2	−3.9	42[e]	0.54	4.8

[a] Determined at η = 123–166 mV. [b] Determined at η = 125–169 mV. [c] Determined at η = 110–152 mV. [d] Determined at η = 120–160 mV. [e] Determined at η = 120–160 mV.

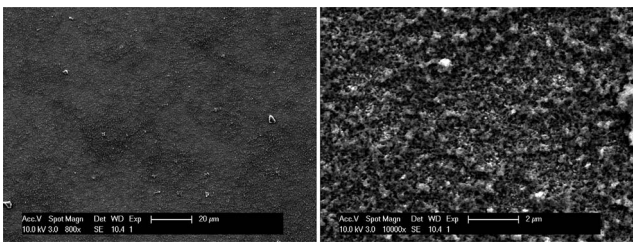

Fig. 7 SEM images of a MoS_3-modified FTO electrode produced by spray-casting. Overview of the modified area (left) and deposited MoS_3 at a higher magnification (right).

electrode assembled by spray-casting. The film is much more uniform than the film made by drop casting. The catalytic activity of these electrodes was studied by polarization measurements (Fig. 8). Again an optimal loading is found, which is 200 μg cm^{-2}. With this loading, the current densities are 0.33 and 2.5 mA cm^{-2} at η = 150 and 200 mV, respectively. The Tafel slopes are 40–45 mV per decade (Table S2, ESI†).

The MoS_3 particles were also deposited onto a glassy carbon electrode using the spray-casting method. Again an optimal loading was found, which is 130 μg cm^{-2} MoS_3 (Fig. S3, ESI†). The current densities at this loading are 0.48 and 4.4 mA cm^{-2} at η = 150 and 200 mV, respectively. The Tafel slopes are about 40 mV per decade (Table S3, ESI†). Addition of MWCNT did not change the catalytic property (Fig. S4, ESI†). This is probably because electron transfer is already efficient for spray-cast electrodes (as indicated by their *ca.* 40 mV per decade Tafel slopes), and therefore MWCNT is no longer needed to decrease the resistance of the electrode.

2.2.3 Modified carbon-paste electrodes. A home-made carbon paste electrode was assembled using 80 wt% synthetic graphite and 20 wt% paraffin wax (Fig. S5, ESI†). HER did not occur at the carbon paste electrode until at a large overpotential (η > 400 mV; line a, Fig. 9). A thin layer of MoS_3 particles was pressed onto the surface of the carbon paste electrode. The resulting MoS_3-sC electrode is now very active for HER (line b, Fig. 9). A catalytic current was visible starting at η = 100 mV. The current densities are 1.0 and 2.7 mA cm^{-2} at η = 150 and 200 mV, respectively.

An electrolysis experiment was conducted using a MoS_3-sC electrode. A stable current density of about 17 mA cm^{-2} was observed over a period of one hour at η = 200 mV and pH = 0 (Fig. 10, top). Thus, the catalyst appears to be stable during electrolysis. The current density here is slightly higher than that determined in the polarization scan. The discrepancy is likely due to the difference in experimental setups, for example, a small variation in the potential.

The amount of hydrogen gas evolved in the electrolysis cell was measured. The Faraday yield of hydrogen production was then calculated. The yield was quantitative during one hour of electrolysis (Fig. 10, bottom). This again indicates the stability of the catalyst.

2.2.4 Comparison of different methods for the fabrication of MoS_3-modified electrodes. Various methods for the fabrication of MoS_3-modified electrodes are compared in Table 3. Glassy carbon is a better substrate than FTO. This might be partially due to a higher resistance of the FTO electrode. In fact, the FTO electrode has a resistance of *ca.* 7 Ω cm^2, while the glassy carbon electrode has a resistance of *ca.* 2 Ω cm^2. Spray-casting produces a more even film than drop casting. As a result, the optimal loading of MoS_3 is higher using the spray-casting technique (200 μg cm^{-2} on FTO and 130 μg cm^{-2} on glassy carbon) than using the drop-casting technique (53 μg cm^{-2} on FTO and 32 μg cm^{-2} on glassy carbon). Thus, it is possible to fabricate a more geometrically active electrode using spray-casting. On the other

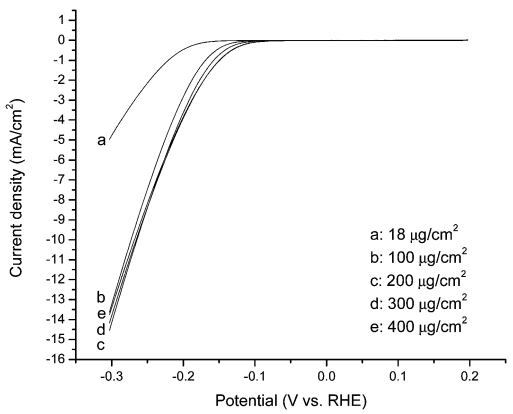

Fig. 8 Polarization curves of spray-cast MoS_3-modified FTO electrodes recorded at pH = 0 (1.0 M H_2SO_4); scan rate: 5 mV s^{-1}.

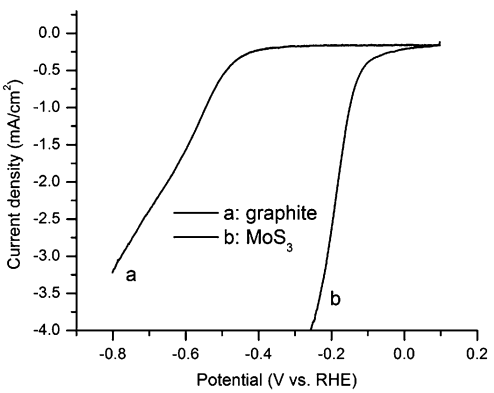

Fig. 9 Polarization curves of blank carbon paste electrode (line a) and MoS_3-modified carbon paste electrodes (line b) recorded at pH = 0 (1.0 M H_2SO_4); scan rate: 5 mV s^{-1}.

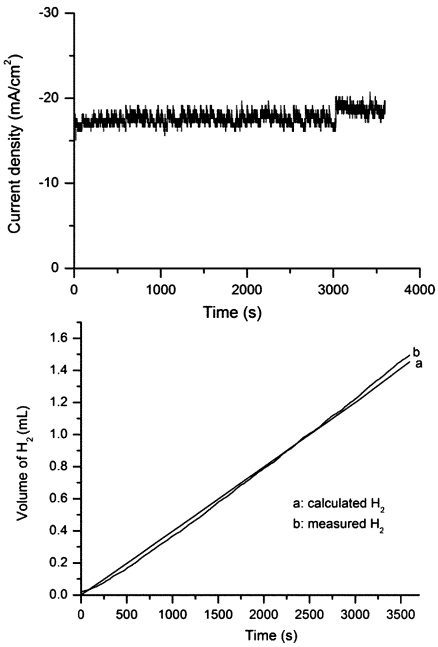

Fig. 10 (Top) Time course of the catalytic current during an electrolysis experiment using a MoS_3-sC electrode. Potential: −200 mV *vs.* RHE; solution: 1.0 M H_2SO_4. (Bottom) Current efficiency for H_2 production catalyzed by a MoS_3-sC electrode. Line a was calculated according to the cumulative charge, assuming a 100% Faraday's yield. Line b is the amount of H_2 measured during electrolysis.

hand, spray-cast electrodes have lower weight-averaged activity compared to their drop-cast counterparts (Table 3). Why a film with better morphology has a lower weight-averaged activity is not clear. The MWCNT is able to significantly improve the activity of MoS_3-modified electrode fabricated by drop casting, but not the electrode fabricated by spray-casting. The MoS_3/MWCNT hybrid electrode produced by drop casting has overall the highest weight-averaged activity and geometric activity. This performance might be attributed to a lower Tafel slope which might result from the high conductivity of MWCNT. The MoS_3-modified carbon paste electrode gives the highest geometric current density at $\eta = 150$; however, it is difficult to calculate its weight-averaged activity. In general, the activity of amorphous MoS_3 particles studied here is significantly higher than previously reported crystalline MoS_2 nanoparticles ($J < 2$ mA cm^{-2} at $\eta = 300$ mV).[5]

Table 3 Comparison of different MoS_3-modified electrodes at optimal loading

Substrate	Casting method	Additive	Loading[a]/ μg cm^{-2}	$j_{\eta=150}$/ mA cm^{-2}	$j_{\eta=200}$/ mA cm^{-2}
FTO	Drop	No	53	0.18	1.1
FTO	Spray	No	200	0.33	2.5
Glassy carbon	Drop	No	32	0.35	2.3
Glassy carbon	Drop	MWCNT[b]	21	0.50	4.8
Glassy carbon	Spray	No	130	0.48	4.4
Glassy carbon	Spray	MWCNT	130	0.48	4.4
Carbon paste	Press	No	Unknown	1.0	2.7

[a] Optimal catalyst loading. [b] MoS_3 : MWCNT = 1 : 2.

2.3 Activation of MoS_3 pre-catalysts

As mentioned in Section 2.2.1, the activity of a freshly prepared MoS_3-modified electrode increases during the first several polarization scans. This happens to the electrodes prepared by different methods. Fig. S2† shows the first six polarization curves for a MoS_3-modified FTO electrode. Apparently there is an activation process for the modified electrodes.

There is a slight possibility that the activity of the modified electrodes is due to Pt contamination. Pt particles might be deposited onto the modified electrodes during polarization scans. To rule out this possibility, the polarization scans were carried out using a Ti counter electrode. The MoS_3-modified FTO electrode shows the same activity and a similar activation process is observed (Fig. S6, ESI†). Thus, the catalytic activity is due to MoS_3 pre-catalysts, not Pt contamination.

A more reasonable cause for the increased activity of the modified electrodes during the first polarization scans is that the MoS_3 pre-catalysts are transformed into the active species during these scans. We reported earlier that for amorphous MoS_3 films deposited by cyclic voltammetry, the MoS_3 species were converted to reduced molybdenum sulfides, possibly amorphous MoS_2, which were the active species.[7] We suspected that a similar reduction occurred with the MoS_3-modified electrodes described here. Indeed, the first polarization curve exhibits a broad reduction peak at potentials more positive than the HER potential (arrow, Fig. 11).

To ascertain that amorphous MoS_3 is reduced after the activation process, a MoS_3-modified FTO electrode subjected to 8 polarization scans until $\eta = 300$ mV was analyzed by XPS (Fig. 12 and S1, ESI†). Some peaks from Sn are visible in the survey spectrum (Fig. S1, ESI†). The Mo ion remains as Mo^{4+} according to the Mo 3d spectrum. There is a noticeable change in the shape of the S 2p spectrum. The relative intensity of the doublet with lower binding energy increases, but the doublet with higher binding energy remains visible. This spectrum is different from that of the electropolymerized MoS_3 film after polarization,

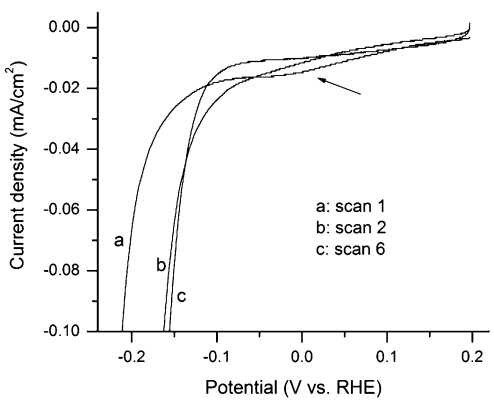

Fig. 11 First polarization curves of freshly prepared MoS_3/FTO electrode recorded at pH = 0 (1.0 M H_2SO_4); scan rate: 5 mV s^{-1}. The electrode was prepared by drop-casting with a loading of 48 μg cm^{-2}.

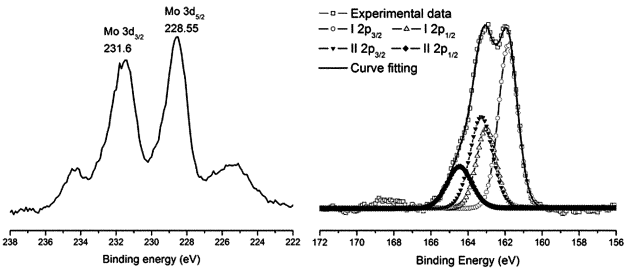

Fig. 12 XPS spectra of the MoS_3-modified electrode after eight polarization measurements. (Left) Mo 3d and S 2s region. (Right) S 2p region; binding energies (eV): doublet I $2p_{3/2}$, 162.0; $2p_{1/2}$, 163.2; doublet II $2p_{3/2}$, 163.3; $2p_{1/2}$, 164.5.

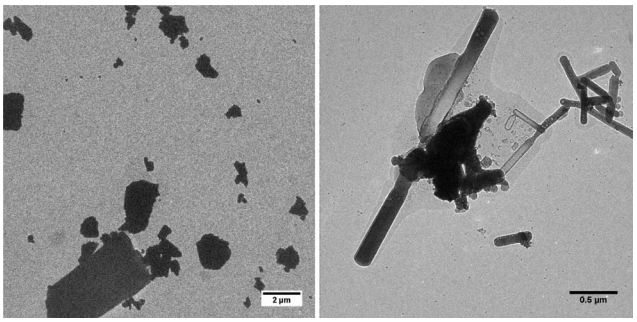

Fig. 13 TEM images of the annealed MoS_x particles. (Left) MoS_3-350. (Right) MoS_2-650.

which shows a single doublet attributable to MoS_2.[7] The spectrum suggests that there are still S_2^{2-} ligands in the current sample. It is possible that only a portion of MoS_3 is reduced to MoS_2 after several polarization scans. To probe this possibility, the MoS_3-modified FTO electrode was subjected to bulk electrolysis for 5 and 10 minutes, respectively. The XPS data of the electrodes after electrolysis are similar to those of the electrode after 8 polarization measurements, showing again two doublets (Fig. S7 and S8, ESI†). These data suggest that the activation process does not convert MoS_3 particles into MoS_2, as is the case for electropolymerized MoS_3 films. Thus, the catalytically active species here is not pure MoS_2, but reduced MoS_x ($x > 2$) species that consists of S_2^{2-} ligands.

This result is consistent with a recent study of amorphous MoS_3 deposited on CdS/CdSe.[8] It was found that MoS_3 could serve as a precatalyst for photolytic hydrogen evolution. Prior to the photocatalysis, the as-deposited MoS_3 was photo-reduced to form reduced species which were the real catalysts. Based on XPS, XANES and EXAFS, the catalyst was identified as a reduced form of MoS_3 rather than MoS_2.[8] It will be interesting to see whether the active catalyst in the MoS_3/CdS system is the same as the active catalyst in the current MoS_3 system. To this end, we are currently exploring more informative characterization tools such as XAS to further probe the structure of the reduced molybdenum sulfide species.

To further elaborate the above-mentioned considerations, we prepared molybdenum sulfide particles by reduction of *in situ* generated MoS_3 species with $NaBH_4$. The XPS data of such molybdenum sulfide species (Fig. S9, ESI†) are similar to those shown in Fig. 12, S7 and S8†. Therefore, this molybdenum sulfide species is not MoS_2, but the same MoS_x species formed by electroreduction of MoS_3 particles. Polarization measurements show that such molybdenum sulfide particles have a similar HER activity as amorphous MoS_3 particles (Fig. S10, ESI†). This result adds further evidence that the active catalyst is reduced MoS_x species when amorphous MoS_3 particles are used as precatalysts.

2.4 Catalytic activity of crystalline MoS_x particles

We found that amorphous MoS_3 particles cannot be reduced by chemical reductants such as hydrazine or hydroxyamine to form MoS_2. The amorphous MoS_3 particles were then annealed to give other forms of molybdenum sulfides. When annealed for 1 h at 350 °C, the particle size increases to about 1 μm (compare Fig. 2 and 13). XPS data and electron diffraction pattern indicate that polycrystalline MoS_3 is formed (MoS_3-350, Fig. S11, ESI†). When annealed for 30 min at 650 °C, the sample is mostly single crystalline MoS_2 (MoS_2-650, Fig. 13 for TEM; Fig. S12, ESI† for XPS and electron diffraction). These particles were pressed onto blank carbon paste electrodes so that their HER activity can be measured (Fig. 14). Both MoS_3-350 and MoS_2-650 exhibit lower activity than MoS_3, with MoS_2-650 being the least active. On the other hand, when MoS_2 micro-crystals (Fig. S13, ESI†; from Aldrich) were used as catalysts, electrochemical hydrogen evolution does not occur until $\eta > 200$ mV (Fig. 14). Thus, for electrocatalytic HER, amorphous MoS_3 particles are the most active catalysts among the various MoS_x particles studied herein.

We[6,7] and others[3] propose that the activity of molybdenum sulfides for hydrogen evolution is due to the presence of unsaturated sulfur atoms in these materials. These sulfur atoms can engage in the discharge reaction and form S–H bonds, which eventually lead to hydrogen formation. The same principle applies here. The MoS_3 particles have a small size and are amorphous. As a result, there are a higher number of unsaturated sulfur atoms at the surface. Annealing leads to a large particle size and higher crystallinity. The amount of unsaturated sulfur atoms decreases, resulting in lower catalytic activity. For the same reason, micro-crystalline MoS_2 particles have the lowest HER activity. This explains the trend observed in Fig. 14.

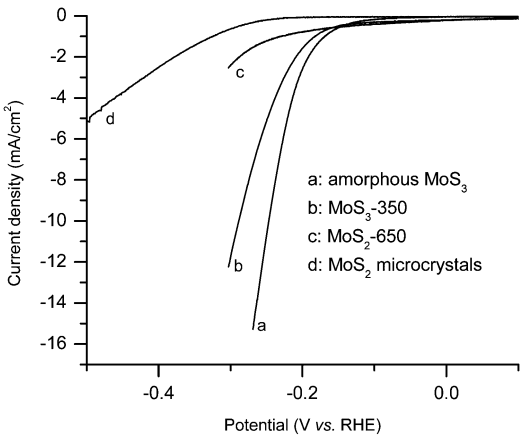

Fig. 14 Polarization curves of carbon paste electrodes modified with a layer of MoS_x-species. The measurements were conducted at pH = 0 (1.0 M H_2SO_4); scan rate: 5 mV s^{-1}.

3. Conclusions

In summary, we describe the synthesis and characterization of amorphous MoS_3 particles, and the fabrication of FTO, glassy carbon, and carbon paste electrodes modified with these MoS_3 particles. The modified electrodes display excellent activity for hydrogen evolution. The work expands our earlier work on electropolymerized MoS_3 films, and provides a new and easy access to amorphous MoS_3 which appears to be a promising non-precious hydrogen evolution catalyst.

A pre-activation process is identified for the amorphous MoS_3 particles. The MoS_3 species are reduced to another form of molybdenum sulfide which still consists of S_2^{2-} ligands. This is different from the observation on electropolymerized MoS_3 films, where MoS_3 is reduced to MoS_2. The work illustrates the complexity in identifying the active species in MoS_x-catalyzed hydrogen evolution.

When the amorphous MoS_3 particles are annealed, MoS_x particles with larger particle size and increased crystallinity are produced. These particles have a lower HER activity compared to MoS_3 particles. It is also found that single-crystalline MoS_2 particles (from commercial sources) are the least active electrocatalysts for HER among all the MoS_x species described herein. This result might be explained by the number of unsaturated sulfur atoms on the surface of these sulfide materials.

4. Experimental

4.1 Chemicals and reagents

All manipulations were carried out under an inert N_2(g) atmosphere using glovebox techniques unless otherwise mentioned. Crystalline MoS_2 particles, synthetic graphite (<20 μm), paraffin wax (mp 50–52 °C) were purchased from Aldrich and used without further purification. Unless noted, all other reagents were purchased from commercial sources and used without further purification.

4.2 Physical methods

GC measurement was conducted on a Perkin-Elmer Clarus 400 GC with a TCD detector and a 5 Å molecular sieves packed column with Ar as a carrier gas. TEM images were taken on a Philips (FEI) CM12 transmission electron microscope with a LaB_6 source operated at 120 kV accelerating voltage. SEM secondary electron (SE) images were taken on a Philips (FEI) XLF-30 FEG scanning electron microscope. Electrochemical measurements were recorded by an IviumStat electrochemical analyzer or an EG&G Princeton Applied Research Potentiostat/Galvanostat model 273. A three-electrode configuration was used. For polarization and electrolysis measurements, a platinum wire was used as the auxiliary electrode and an Ag/AgCl (KCl saturated) electrode was used as the reference electrode. The reference electrode was placed in a position very close to the working electrode with the aid of a Luggin tube. Potentials were referenced to a reversible hydrogen electrode (RHE) by adding a value of (0.197 + 0.059 pH) V. Ohmic drop correction was done prior to Tafel analysis. Pressure measurements during electrolysis were performed using a SensorTechnics BSDX0500D4R differential pressure transducer. Both current and pressure data were recorded simultaneously using an A/D Labjack U12 interface with a sampling interval of one point per second. X-Ray photoelectron spectroscopy (XPS) data were collected by an Axis Ultra (Kratos Analytical, Manchester, UK) under ultra-high vacuum conditions (<10^{-8} Torr), using a monochromatic Al K_α X-ray source (1486.6 eV), in the Surface Analysis Laboratory of CIME at EPFL. The source power was maintained at 150 W (10 mA, 15 kV). Gold (Au $4f_{7/2}$) and copper (Cu $2p_{3/2}$) lines at 84.0 and 932.6 eV, respectively, were used for calibration, and the adventitious carbon 1s peak at 285 eV as an internal standard to compensate for any charging effects. For quantification, relative sensitivity factors from the supplier were used. The XPS samples were placed inside an antechamber which was then evacuated by an independent turbomolecular pump. The inner door of the antechamber was then opened and the samples were introduced to the main chamber for XPS analysis.

4.3 Preparation of MoS_3 particles

In a typical preparation, molybdenum trioxide (1.0 g, 6.95 mmol) was added to an aqueous solution of sodium sulfide (8.34 g, 34.74 mmol of $Na_2S \cdot 9H_2O$ in 250 mL of water) to form a bright yellow solution. This solution was then kept under vigorous stirring while 6.0 M aqueous HCl was added slowly (~10 minutes) until the solution reached a pH of 4. At first, darkening of the solution was observed; close to the end of the addition, a large amount of gaseous H_2S was produced. After the addition of acid, the solution was boiled for 30 minutes to remove the H_2S present in solution and to improve the filtration step. After being cooled to ambient temperature, the solution was filtered under vacuum and washed with a copious amount of water and then ethanol.

The moist dark paste obtained was then transferred to an Erlenmeyer flask and 1.0 L of acetone was added, and the mixture was stirred for 30 minutes. The suspension was then sonicated for 5 minutes using an ultrasonic horn at 20 kHz. A clear brown sol was obtained and it was stable for at least 3 days without precipitation. If coagulation of the sol was visible, it could be sonicated again to yield a clear sol.

When powdered MoS_3 was desired, the dark paste obtained after filtration was oven dried for 12 h at 80 °C to yield a black vitreous solid that could be powdered with the aid of a mortar.

4.4 Preparation of MoS_3 modified FTO electrodes by drop casting

The stock MoS_3 sol was used to obtain MoS_3 modified electrodes using the drop-coating technique. The concentration of the sol was around 0.4 g L^{-1}, determined gravimetrically by weighing the solid residue after evaporation of the solvent for a 1 mL aliquot. A drop (10 μL) of the stock sol solution was added on the conductive surface of FTO coated glass (which was thoroughly cleaned with ethanol prior to use), and was then allowed to dry in air. More drops could be added consecutively on the same spot, but only after the solvent from the previous drop(s) had evaporated. Electrodes with MoS_3-loadings of 13 μg cm^{-2}, 27 μg cm^{-2}, 40 μg cm^{-2}, and 53 μg cm^{-2} were prepared by drop casting 1, 2, 3 or 4 drops, respectively. The electrode with the loading of 75 μg cm^{-2} was prepared by drop casting one drop

(10 μL) of a MoS_3 sol of 1.8 g L^{-1}. Prior to drop casting, the suspensions were sonicated for several minutes.

4.5 Preparation of MoS_3 modified glassy carbon electrodes by drop casting

The electrodes (*ALS*) were polished with two different alpha alumina powders (1.0 and 0.3 micron from *CH Instruments*) suspended in distilled water on a Nylon polishing pad (*CH Instruments*) and with gamma alumina powder (0.05 micron from *CH Instruments*) suspended in distilled water on a Microcloth polishing pad (*CH Instruments*). Before going to the next smaller powder size and at the end of polishing, the electrodes were thoroughly rinsed with distilled water. 10 μL of MoS_3 sol in EtOH (various concentrations), occasionally containing different amounts of MWCNTs, were drop cast on a glassy carbon disk electrode and the solvent was allowed to evaporate at room temperature. The diameter of the glassy carbon disk is 3 mm, whereas the diameter of the whole electrode is 6 mm. Therefore, one-fourth of the surface is glassy carbon, *i.e. ca.* ¼ of the total loading will be on the glassy carbon.

The mixtures of MoS_3 particles with MWCNTs (carbon nanotubes, multiwalled; purchased from Aldrich) were prepared as follows. 0.5 mL of MoS_3 suspension in EtOH (1.8 mg mL^{-1}) were mixed with increasing amounts of MWCNT suspension in EtOH (1.8 mg mL^{-1}). EtOH was added to the resulting mixture to have a final total volume of 1.5 mL. Mixtures with MoS_3/MWCNT weight ratios of 1 : 0.4 ("additional 40 wt% MWCNTs"), 1 : 1 (100 wt%), 1 : 1.6 (160 wt%) and 1 : 2 (200 wt %) were prepared. Prior to drop casting, the suspensions were sonicated for several minutes.

4.6 Preparation of MoS_3 modified FTO electrodes by spray casting

20 μL of MoS_3 sol in EtOH (various concentrations) were spray cast on a FTO coated glass plate (which was thoroughly cleaned with ethanol prior to use) with an airbrush (from *Revell*, compressor pressure ≈ 1 bar). The whole amount of sol was sprayed on a defined area of 0.2 cm^2. Prior to spray casting, the suspensions were sonicated for several minutes.

4.7 Preparation of MoS_3 modified glassy carbon electrodes by spray casting

The glassy carbon electrodes were cleaned and polished as described above. 10 μL of MoS_3 sol in EtOH (various concentrations), occasionally containing different amounts of MWCNTs, were spray cast on a glassy carbon electrode with an airbrush (from *Revell*, compressor pressure ≈ 1 bar). The whole amount of sol was tried to be sprayed on the glassy carbon surface only. However, a minor loss of material due to deposition on the plastic covering of the electrode could not be excluded. The suspensions containing MWCNTs were prepared as described above. Prior to spray casting, the suspensions were sonicated for several minutes.

4.8 Preparation of carbon paste electrodes

8 g of powdered synthetic graphite (<20 μm) and 2 g of white paraffin wax were placed in a round-bottom flask. 40 mL of hot toluene was added to the flask. The mixture was sonicated in an ultrasonic bath for 5 minutes. The solvent of the resulting solution was removed under vacuum to yield a conductive graphite powder. The powder was pressed to fill the empty body of a home-made electrode, to give the carbon paste electrode (Fig. S5, ESI†).

4.9 Preparation of MoS_x-modified carbon paste electrodes

The surface of the carbon paste electrode was cleaned using weighing paper. Powdered MoS_x particles were then pressed against the soft surface of the carbon paste electrode and were spread evenly on the surface using weighing paper (MoS_x includes MoS_3, MoS_3-350, MoS_2-650, and MoS_2). The commercial MoS_2 particles are crystalline, as shown by TEM and electron diffraction studies.

4.10 Preparation of MoS_x species by reduction with $NaBH_4$

Sodium borohydride (0.10 g, 2.64 mmol) was added at once into an aqueous solution of ammonium tetrathiomolybdate (0.5 g, 1.92 mmol in 100 mL of water). H_2 gas and a black precipitate formed immediately. The reaction mixture was kept stirring for 10 minutes, and then 5 mL of pure acetic acid was added to quench the remaining borohydride reagent. The mixture was then heated at 100 °C for 15 minutes, filtered when it was still hot, and washed with water and then ethanol.

The moist dark paste obtained was then transferred to an Erlenmeyer flask and 400 mL of acetone was added, and the mixture was stirred for 30 minutes. The suspension was then sonicated for 5 minutes using an ultrasonic horn at 20 kHz. A clear brown sol was obtained with an approximate concentration of 0.8 g L^{-1}.

4.11 Preparation of MoS_3-350 and MoS_2-650 particles

Dry powdered MoS_3 was annealed in a quartz tube (5 mm I.D. 250 mm) in a tubular furnace. For the samples annealed at 350 °C, 0.5 g of MoS_3 was placed in the middle of the quartz tube between two small pieces of quartz wool and the tube was inserted in the hot tubular furnace and heated for one hour while purging with a small flow of nitrogen gas. For the sample annealed at 650 °C, 0.5 g of MoS_3 was added to the bottom of the tube and covered with a small piece of quartz wool. The tube was evacuated overnight to remove traces of moisture and sealed under vacuum. The bottom of the tube containing the sample was inserted in the hot tubular furnace and heated for 30 minutes. Elemental sulfur sublimates into the cold part of the tube in the first few minutes of heating. After 30 minutes the tube was left to cool to room temperature and broken to remove the product.

4.12 Tafel measurements and analysis

For Tafel analysis, polarization curves were measured in 1.0 M H_2SO_4 in water with a scan rate of 1 mV s^{-1}. The Pt counter electrode, the Ag/AgCl reference electrode and the working electrode were not separated. The logarithm of the negative current density of the resulting polarization curve was plotted *vs.* overpotential.

Tafel analysis was made with the data, where the curve showed linear behavior. Therefore, the range of overpotential taken for Tafel analysis can vary between different samples.

4.13 Electrolysis

Electrolysis experiments were performed in an H shaped cell. The platinum counter electrode was separated from the solution through a porous glass frit (porosity 3) and this whole assembly was inserted into one side of the H cell. The modified working electrode was inserted in the other side of the cell, together with a magnetic stirring bar and a Luggin capillary. Two small inlets were present in the cell allowing the connection to the pressure monitoring device and the other kept closed by a septum for sampling of the gas phase. The whole cell apparatus is gas-tight and the pressure increase is proportional to the gases generated ($H_2 + O_2$). It is assumed that for 2 moles of H_2 generated in the working electrode, 1 mole of O_2 is generated in the counter electrode. Prior to each experiment, the assembled cell was calibrated by injecting known amounts of air into the closed system and recording the pressure change, and after the calibration the cell was purged with nitrogen for 20 minutes and the measurements were performed.

Control experiments were performed using platinum as a working electrode and a quantitative Faraday yield was obtained by measuring the pressure (97–102%) and confirmed by GC analysis of the gas in the headspace (92–96%) at the end of the electrolysis.

Acknowledgements

This work is supported by a starting grant from the European Research Council under the European Community's Seventh Framework Programme (FP7 2007-2013)/ERC grant agreement no. 257096.

Notes and references

1 M. G. Walter, E. L. Warren, J. R. McKone, S. W. Boettcher, Q. X. Mi, E. A. Santori and N. S. Lewis, *Chem. Rev.*, 2010, **110**, 6446–6473; T. R. Cook, D. K. Dogutan, S. Y. Reece, Y. Surendranath, T. S. Teets and D. G. Nocera, *Chem. Rev.*, 2010, **110**, 6474–6502; V. Artero and M. Fontecave, *Coord. Chem. Rev.*, 2005, **249**, 1518–1535; J. A. Cracknell, K. A. Vincent and F. A. Armstrong, *Chem. Rev.*, 2008, **108**, 2439–2461; M. R. DuBois and D. L. DuBois, *Chem. Soc. Rev.*, 2009, **38**, 62–72; M. M. Jaksic, *Electrochim. Acta*, 2000, **45**, 4085–4099; A. M. Appel, D. L. DuBois and M. R. DuBois, *J. Am. Chem. Soc.*, 2005, **127**, 12717–12726; M. Razavet, V. Artero and M. Fontecave, *Inorg. Chem.*, 2005, **44**, 4786–4795; X. L. Hu, B. M. Cossairt, B. S. Brunschwig, N. S. Lewis and J. C. Peters, *Chem. Commun.*, 2005, 4723–4725; X. L. Hu, B. S. Brunschwig and J. C. Peters, *J. Am. Chem. Soc.*, 2007, **129**, 8988–8998; H. I. Karunadasa, C. J. Chang and J. R. Long, *Nature*, 2010, **464**, 1329–1333; M. L. Helm, M. P. Stewart, R. M. Bullock, M. R. DuBois and D. L. DuBois, *Science*, 2011, **333**, 863–866.

2 E. Navarro-Flores, Z. W. Chong and S. Omanovic, *J. Mol. Catal. A: Chem.*, 2005, **226**, 179–197; B. Winther-Jensen, K. Fraser, C. Ong, M. Forsyth and D. R. MacFarlane, *Adv. Mater.*, 2010, **22**, 1727–1730; A. Le Goff, V. Artero, B. Jousselme, P. D. Tran, N. Guillet, R. Metaye, A. Fihri, S. Palacin and M. Fontecave, *Science*, 2009, **326**, 1384–1387; P. D. Tran, A. Le Goff, H. J. B. Jousselme, N. Guillet, S. Palacin, H. Dau, M. Fontecave and V. Artero, *Angew. Chem., Int. Ed.*, 2011, **50**, 1371–1374.

3 T. F. Jaramillo, K. P. Jorgensen, J. Bonde, J. H. Nielsen, S. Horch and I. Chorkendorff, *Science*, 2007, **317**, 100–102.

4 B. Hinnemann, P. G. Moses, J. Bonde, K. P. Jorgensen, J. H. Nielsen, S. Horch, I. Chorkendorff and J. K. Norskov, *J. Am. Chem. Soc.*, 2005, **127**, 5308–5309; T. F. Jaramillo, J. Bonde, J. D. Zhang, B. L. Ooi, K. Andersson, J. Ulstrup and I. Chorkendorff, *J. Phys. Chem. C*, 2008, **112**, 17492–17498; X. Zong, H. J. Yan, G. P. Wu, G. J. Ma, F. Y. Wen, L. Wang and C. Li, *J. Am. Chem. Soc.*, 2008, **130**, 7176–7177; Y. G. Li, H. L. Wang, L. M. Xie, Y. Y. Liang, G. S. Hong and H. J. Dai, *J. Am. Chem. Soc.*, 2011, **133**, 7296–7299.

5 J. Bonde, P. G. Moses, T. F. Jaramillo, J. K. Norskov and I. Chorkendorff, *Faraday Discuss.*, 2009, **140**, 219–231.

6 D. Merki and X. L. Hu, *Energy Environ. Sci.*, 2011, **4**, 3878–3888.

7 D. Merki, S. Fierro, H. Vrubel and X. L. Hu, *Chem. Sci.*, 2011, **2**, 1262–1267.

8 M. L. Tang, D. C. Grauer, B. Lassalle-Kaiser, V. K. Yachandra, L. Amirav, J. R. Long, J. Yano and A. P. Alivisatos, *Angew. Chem., Int. Ed.*, 2011, **50**, 10203–10207.

9 G. Krüss, *Justus Liebigs Ann. Chem.*, 1884, **225**, 1–57; Z. Z. Wu, D. Z. Wang and A. K. Sun, *J. Mater. Sci.*, 2010, **45**, 182–187.

10 T. Weber, J. C. Muijsers and J. W. Niemantsverdriet, *J. Phys. Chem.*, 1995, **99**, 9194–9200.

11 J. C. Muijsers, T. Weber, R. M. vanHardeveld, H. W. Zandbergen and J. W. Niemantsverdriet, *J. Catal.*, 1995, **157**, 698–705.

